An Analog VLSI Velocity Sensor

Jörg Kramer, Rahul Sarpeshkar and Christof Koch

California Institute of Technology
Computation and Neural Systems 139-74
Pasadena, CA 91125
phone: (818) 395-2874
fax: (818) 796-8876
e-mail: kramer@cns.caltech.edu

ABSTRACT

An integrated circuit that computes the velocity vector of a visual stimulus in one dimension is presented. The circuit combines optical sensors and associated electronics on a single silicon chip, processed with standard CMOS technology. The velocity is inferred from the time delay of the appearance of an image feature at two fixed locations on the chip. The circuit operates quite robustly for high-contrast stimuli over considerable irradiance and velocity ranges. With lower-contrast stimuli the output signal for a given velocity tends to decrease, while the direction selectivity is still maintained. The individual motion-sensing cells are compact, and they are therefore suited for use in dense 1D or 2D imaging arrays.

I. INTRODUCTION

Various applications in robotic guidance and remote sensing require small, fast, sensors for the processing of visual motion. Robust measurement of velocity in real time is a difficult task, but necessary if a system has to operate in dynamic environments. Parallel processing at each image location is best suited to handle the large volume of incoming irradiance data from the optical sensors. The processed output should neither depend on irradiance nor on contrast. However, because physical systems are always subject to the presence of noise, the output is a function of these parameters, even in high-performance biological systems like the fly.

In this article, an elementary sensor for the determination of 1D velocity in real time is reported. It is constructed by combining photoreceptors with analog electronic circuitry on a single silicon substrate using CMOS VLSI technology. Analog integrated circuits do not attain the precision levels of digital circuits, but they are better suited to meet the criteria of compactness and low power consumption. Parallel processing and real-time operation are achieved by building arrays from these elementary motion sensors. Previous attempts at implementing 1D or 2D motion sensors with analog VLSI technology have been made [1-4]. None of these circuits outputs a signal that unambiguously encodes velocity independently of image brightness and contrast over typical ranges encountered in natural scenes.

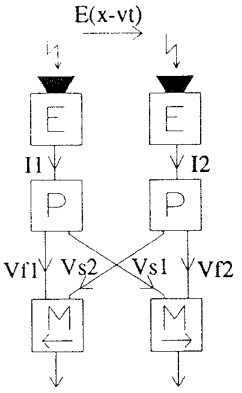

Fig. 1. Architecture of the motion sensor. Temporal edge detectors (E) generate short current spikes in response to fast image irradiance (i.e. brightness) transients. Pulse shaping circuits (P) convert the current spikes into voltage pulses. Voltage pulses from adjacent pixels are fed into motion circuits (M) computing velocity in one dimension.

The circuit presented here exhibits a monotonic dependence of the output signal on the 1D stimulus velocity. It operates robustly over large speed and illumination ranges. It is more compact and responds to lower contrasts than most previous implementations. It uses the architecture schematically illustrated in Figure 1. At each pixel location, a quick irradiance transient is converted into a short current spike by a temporal edge detector (E). This current spike is transformed into two different voltage pulses by a pulse shaping circuit (P). Each one of these voltage pulses, together with the other voltage pulse

0-7803-2570-2/95 $4.00 ©1995 IEEE

of the adjacent pixel, is fed into a motion circuit (M) that responds to one direction of motion; the pair of motion circuits responds to both directions of motion. Note that a single motion sensor in a 1D array contains a pair of motion circuits, but only one edge detector and one pulse shaping circuit; this is so, because the pulse outputs are used by neighboring motion sensors as well.

II. TEMPORAL EDGE DETECTOR

The motion sensor uses a temporal edge detector as an input stage. At each pixel site a rapid increase in brightness is converted into a short current spike. This corresponds to detection of temporal dark-bright or ON edges. The circuit schematic is shown in Figure 2.

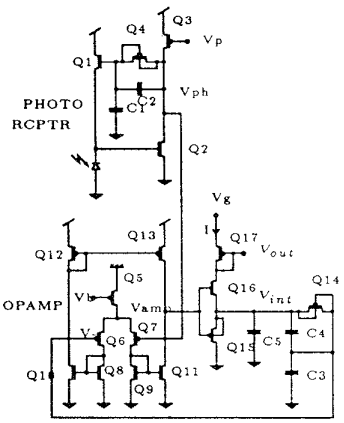

Fig. 2. Circuit diagram of the edge detector, consisting of a photoreceptor, and a "haircell" with amplification, differentiation, and rectification.

The adaptive photoreceptor (Q_1–Q_4) was developed by Delbrück [3]. Its output voltage V_{ph} increases logarithmically with irradiance of the photodiode, as long as the MOSFETs are operated below threshold. Thus, a transient dE in the image irradiance E causes a voltage transient dV_{ph} that is only a function of contrast dE/E. This property is highly desirable for the extraction of local features from an image, because the overall illumination of a typical scene is likely to change with time. The transient step response is higher than the adapted DC response by $(C_1+C_2)/C_2$, the inverse of the capacitive divider gain in the feedback loop. The I-V relationship of the adaptive element Q_4 is that of a sinh. Consequently, the adaptation is slow for small output voltage steps and fast for large steps. With $(C_1 + C_2)/C_2 = 10$, adaptation time constants of several seconds were obtained. In subthreshold operation, the transient change of the photoreceptor output voltage to an irradiance step is given by

$$dV_{ph} = \left(\frac{kT}{q\kappa}\right)\left(\frac{C_1+C_2}{C_2}\right)\left(\frac{dE}{E}\right) \quad (1)$$

where kT/q is the thermal voltage and κ is the back-gate coefficient of Q_1.

The output of the photoreceptor is fed into a circuit that transduces positive voltage excursions in the photoreceptor voltage, corresponding to ON edges, to a current. The transistors Q_5–Q_{13} comprise a wide-range operational amplifier with a bias V_b, connected to some other transistors (Q_{14}–Q_{17}) and capacitors (C_3–C_5), so that it is in a non-inverting feedback configuration. The capacitors C_3 and C_4 form a capacitive divider that causes the gain of V_{int} to be $(C_3+C_4)/C_4$ with respect to the input voltage V_{ph} of the amplifier. The adaptive element Q_{14} is a sinh element, identical to that used in the photoreceptor, that prevents the V_- node of the amplifier from floating by slowly adapting it to V_{int}. The current charging the node V_{int} is given by

$$I = C_{tot}dV_{int}/dt, \quad (2)$$

where

$$C_{tot} = C_5 + \frac{C_3C_4}{C_3+C_4}, \quad (3)$$

if we make the assumption that Q_{14} is only weakly turned on. This current is supplied by Q_{16} if it is positive and by Q_{15} if it is negative. The transistor Q_{15} is source-connected to minimize body-effects, since the DC voltages of operation are around 1.5 V. If we sense the current in Q_{16} with the diode-connected Q_{17}, V_{out} may be used to mirror copies of it to succeeding circuits. The voltage V_g may be used to set the gain of this output mirror if it is operated within a few mV of V_{DD}. The circuit thus serves as a differentiating, amplifying, and half-wave-rectifying element all-in-one. It is a functional analog of auditory hair cells that sense the motion of the basilar membrane in the cochlea. Here, it is used to sense voltage changes in the photoreceptor output caused by irradiance increases. Using (1)–(3) we can calculate the net output current as

$$I = C_{tot}\left(\frac{C_3+C_4}{C_4}\right)\left(\frac{C_1+C_2}{C_2}\right)\left(\frac{kT}{q\kappa}\right)\left(\frac{dE}{Edt}\right). \quad (4)$$

The output current is therefore proportional to the temporal contrast $\left(\frac{dE}{Edt}\right)$. The temporal contrast is the product of the velocity v and the spatial contrast $\left(\frac{dE}{Edx}\right)$

$$\frac{dE}{Edt} = v\frac{dE}{Edx}. \quad (5)$$

III. PULSE SHAPING CIRCUIT

The circuit shown in Figure 3(a) is a nonlinear version of a differentiator constructed by having a low-pass filter in the feedback path of a high-gain amplifier. The transistors Q_{20}–Q_{22} and capacitor C function as a source-follower-like low-pass filter; the high-gain amplifier is formed by

Q_{18} and Q_{19}. The input to the circuit is a current I, obtained from the mirror constructed by connecting the output voltage of the edge detector (V_{out} in Figure 2) to V_{in} of the filtering circuit. The voltage V_f responds to an input current spike from the edge detector with a voltage spike. The voltage V_s responds to the same spike with a sharp onset and a $\log(t)$-like decay. The input I may be thought of as an impulse that sets the initial condition on the diode-capacitor subcircuit of Q_{21}, Q_{22}, and C. It may be shown that, for an initial condition with a spike height of I_{in}, the diode-capacitor current I_{out} is given by

$$I_{out}(t) = \frac{I_{in}}{1 + \frac{I_{in}t}{CV_C}}, \tag{6}$$

where

$$V_C = \frac{kT(\kappa + l)}{q\kappa^2}. \tag{7}$$

The voltage V_C obtained by using two stacked diodes is larger than that obtained by using one diode, and serves to increase V_f and V_s. After a sufficiently long time t, such that $I_{in}t >> CV_C$, $I_{out}(t) \sim CV_C/t$ and $V_s(t) \sim V_C \log(t)$, i.e. I_{out} and V_s are *independent of* I_{in}. Conversely, at a given time t_d, $I(t_d) \sim CV_C/t$ if $I_{in}t_d >> CV_C$. We shall explain in section IV how we exploit this property to make our velocity output independent of contrast, if the contrast is sufficiently large. Note that a diode-capacitor configuration intrinsically adapts to time constants over many orders of magnitude. Therefore, the circuit has no explicit time constant determined by a bias voltage, nor does it have an explicit threshold for the value of I_{in} where contrast-insensitivity begins.

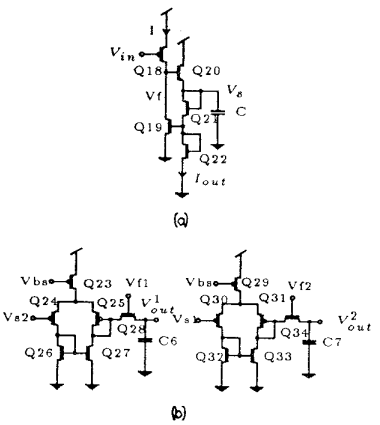

Fig. 3. Circuit diagrams of (a) the pulse shaping circuit generating two voltage pulses V_f and V_s in response to a current pulse I, and (b) a pair of motion circuits computing speed in opposite directions. The voltage terminals V_{f1} and V_{s1} refer to the outputs of one pulse shaping circuit, while V_{f2} and V_{s2} refer to those of the other one, as indicated in Fig. 1.

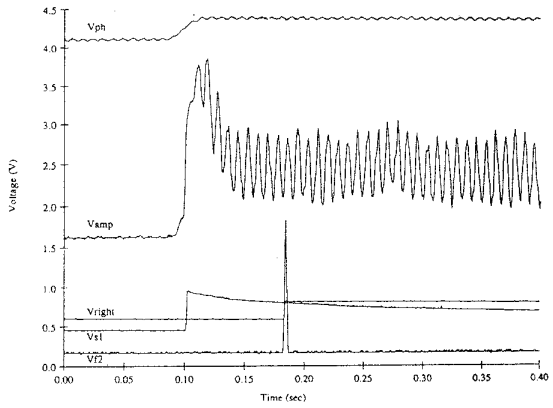

Fig. 4. Output voltage traces of different stages of the motion sensing circuit in response to a moving black bar on a white background. The top trace is the photoreceptor output V_{ph}. The central trace is the output of the wide-range amplifier V_{amp}. The bottom traces are the slowly-decaying facilitation pulse V_{s2}, the short sampling pulse V_{f1} from the adjacent pixel in the preferred direction, and the sampled output V^1_{out}. For better visibility, the V_{ph} trace and the V_{amp} trace are offset by 3 V and 1 V respectively. Note that the flicker noise of the incandescent lighting can clearly be seen on the V_{amp} trace. The delay of V_f with respect to V_s, relevant for the computation of velocity, is about 80 ms.

IV. MOTION CIRCUITS

For the computation of the velocity of a stimulus the analog voltage of the slowly decaying pulse V_s initiated at one pixel is sampled by the voltage spike V_f triggered at an adjacent pixel. For the determination of a signed velocity component, two such sample-and-hold circuits are necessary (Figure 3(b)); this is so because each circuit can only determine speed for the direction of motion where the V_s pulse is initiated before the V_f spike. This direction is called the preferred direction. Since the V_s pulse facilitates the measurement, we call the algorithm facilitate-and-sample (FS). The monotonic decay of the facilitation pulse ensures unambiguous encoding of speed in the sampled voltage. In the other direction, called the null direction, the sampling pulse precedes the facilitation pulse and the voltage of the facilitation pulse triggered by the previous edge is sampled. The latter voltage is normally low unless edges arrive in quick succession. The FS circuit responds down to arbitrarily slow speeds, while showing good sensitivity at high speeds. Under the assumption that $I_{in}\Delta x/v >> CV_C$, where Δx is the pixel spacing, the sampled output voltage V_{out} is independent of I_{in} and is given by $V_{out} \sim V_C \log\left(\frac{\Delta x}{v}\right)$. The sensitivity dV_{out}/dv is highest at slow speeds, decaying with v^{-1}. A single element of our velocity sensor consisting of a temporal edge detector, a pulse shaping circuit, and two motion circuits comprises 34 transistors.

V. EXPERIMENTAL RESULTS

The FS motion sensor was fabricated using a 2 μm n-well CMOS process provided by MOSIS. An elementary

motion cell covers an area of 0.05 mm^2. The imaging lens used for circuit testing has a focal length $f = 13$ mm and an f-number of 1.8. For quantitative measurements, sheets of paper with printed gray scale patterns were wrapped around a rotating drum to provide the optical stimuli. The object distance was set to 380 mm. Measurements were taken under incandescent room lighting conditions, where a white paper surface provided an illuminance of about 1.2 lux on the chip. Figure 4 shows the response of the different stages of the circuit to a black moving bar on a white background. The 120 Hz flicker noise can clearly be seen on the ouptut voltage trace V_{amp} of the wide-range amplifier. The bias of the operational amplifier V_b was set at low gain (low V_b) so that the flicker noise remained tolerable.

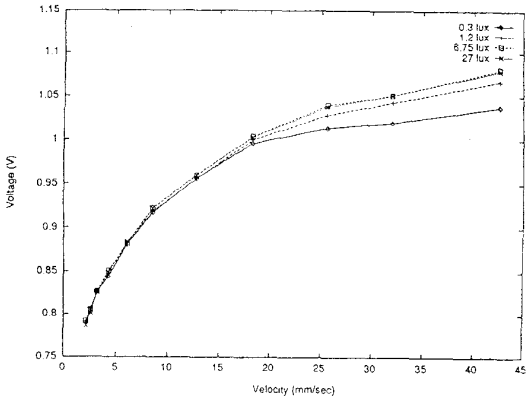

Fig. 5. Output voltage of a direction-selective motion sensing element versus velocity caused by motion in the preferred direction for different incandescent illumination levels. The pixel spacing of 300 μm corresponds to an optical angle of 1.28° and a distance of 8.5 mm on the object. Each data point represents the average of 5 successive measurements.

The response curves for the preferred direction at different global illumination levels are shown in Figure 5. The proximity of the curves to each other is a result of the good contrast encoding of the photoreceptor. Robust operation was observed down to very dim room illumination levels. In Figure 6, the effect of using different edge sharpnesses and contrasts under standard room lighting conditions is shown. The decrease of the response at relatively high contrasts is due to the fact that the input stage had to be operated at low gain in order to suppress flicker noise. Experiments with DC illumination show that a 40% contrast sinusoidal stimulus can be made to yield almost the same response as a 100% contrast bar stimulus.

VI. CONCLUSION

An algorithm for the measurement of velocity in one dimension and an implementation with analog circuitry using CMOS VLSI technology was presented. The circuit is more compact and more reliable than any previously reported analog single chip velocity sensors, the authors are aware of. It operates robustly over more than one order of magnitude in velocity, is contrast-invariant for sufficiently high contrasts while gradually degrading at low contrasts, and works down to dim room light levels.

ACKNOWLEDGMENT

This work was supported by grants from the Swiss National Science Foundation and the Office of Naval Research. Fabrication of the integrated circuits was provided by MOSIS.

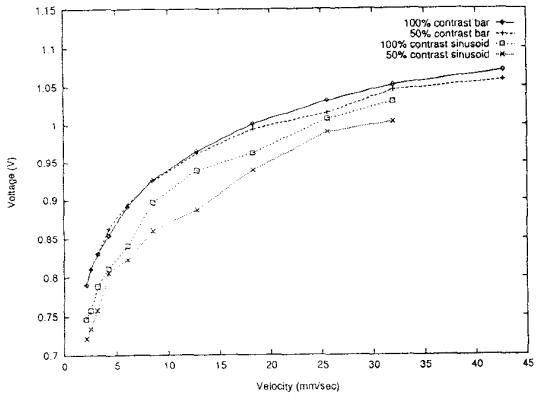

Fig. 6. Output voltage of a direction-selective motion sensing element versus velocity caused by motion in the preferred direction for bar and sinusoidal stimuli of different contrasts. Each data point represents the average of 5 successive measurements under incandescent room illumination.

REFERENCES

[1] J. Tanner and C. Mead, " An Integrated Analog Optical Motion Sensor," in *VLSI Signal Processing, II*, S. Y. Kung, Ed. New York: IEEE Press, 1986, pp. 59-76.

[2] T. Horiuchi, W. Bair, B. Bishofberger, J. Lazzaro and C. Koch, "Computing motion using analog VLSI chips: an experimental comparison among different approaches," *Int. J. Comp. Vision*, vol. 8, pp. 203-216, 1992.

[3] T. Delbrück, "Investigations of analog VLSI visual transduction and motion processing," Ph.D. dissertation, Department of Computation and Neural Systems, California Institute of Technology, Pasadena, CA, 1993.

[4] R. Sarpeshkar, W. Bair and C. Koch, "Visual Motion Computation in Analog VLSI using Pulses," in *Advances in Neural Information Processing Systems 5*, D. S. Touretzky, Ed. San Mateo, CA: Morgan Kaufman, 1993, pp. 781-788.